ACS Catalysis

Article

Exploring the Scope of an #/#-Aminomutase for the Amination of Cinnamate Epoxides to Arylserines and Arylisoserines

Prakash Kumar Shee, Nishanka Dilini Ratnayake, Tyler Walter, Olivia Goethe, Edith N Onyeozili, and Kevin D Walker

ACS Catal., **Just Accepted Manuscript** • DOI: 10.1021/acscatal.9b01557 • Publication Date (Web): 09 Jul 2019

Exploring the Scope of an α/β-Aminomutase for the Amination of Cinnamate Epoxides to Arylserines and Arylisoserines

Prakash K. Shee,[†] Nishanka Dilini Ratnayake,[†] Tyler Walter,[†] Olivia Goethe,[†] Edith Ndubuaku Onyeozili,[§] and Kevin D. Walker[*,†,‡]

† Department of Chemistry, Michigan State University, East Lansing, Michigan 48824, United States

‡ Department of Biochemistry and Molecular Biology, Michigan State University, East Lansing, Michigan, 48824, United States

§ Department of Chemistry, Florida Agricultural & Mechanical University, Tallahassee, Florida 32307, United States

Abstract: Biocatalytic process-development continues to advance toward discovering alternative transformation reactions to synthesize fine chemicals. Here, a 5-methylidene-3,5-dihydro-4*H*-imidazol-4-one (MIO)-dependent phenylalanine aminomutase from *Taxus canadensis* (*Tc*PAM) was repurposed to irreversibly biocatalyze an intermolecular amine transfer reaction that converted ring-substituted *trans*-cinnamate epoxide racemates to their corresponding arylserines. From among twelve substrates, the aminomutase ring-opened 3'-Cl-cinnamate epoxide to 3'-Cl-phenylserine 140 times faster than it opened the 4'-Cl-isomer, which was turned over slowest among all epoxides tested. GC/MS analysis of chiral auxiliary derivatives of the biocatalyzed phenylserine analogues showed that the *Tc*PAM-transamination reaction opened the epoxides enantio- and diastereoselectively. Each product mixture contained (2*S*)+(2*R*)-*anti* (*erythro*) and (2*S*)+(2*R*)-*syn* (*threo*) pairs with the *anti*-isomers predominating (~90:10 dr). Integrating the vicinal proton signals in the ^{1}H-NMR spectrum of the enzyme-catalyzed phenylserines and calculating the chemical shift difference (Δδ) between the *anti* and *syn* proton signals confirmed the diastereomeric ratios and relative stereochemistries. Application of a (2*S*)-threonine aldolase from *E. coli* further established the absolute stereochemistry of the chiral derivatives of the diastereomeric enzymatically derived products. The 2*R*:2*S* ratio for the biocatalyzed *anti*-isomers was highest (88:12) for 3'-NO_2-phenylserine and lowest (66:34) for 4'-F-phenylserine. This showed that the stereospecificity of *Tc*PAM is in part directed by the substituent-type on the cinnamate epoxide analogue. The catalyst also converted each cinnamate epoxide analogue to its corresponding *iso*serine, highlighting a biocatalytic route to arylisoserines, which play a key role in building the pharmacophore seen in anticancer and protease inhibitor drugs.

Keywords: biocatalysis, MIO-aminomutase, phenylisoserine, phenylserine, cinnamate epoxides, enzyme catalysis

INTRODUCTION

Nonproteinogenic amino acids are a specialized class of organic compounds that often have intrinsic biological activity.[1-4] More frequently, these vital amino acids are found in peptides with antiviral,[5] antitumor,[6] anti-inflammatory,[7] or immunosuppressive activities.[8] β-Hydroxy-α-amino acids reside in an important subclass of nonproteinogenic amino acids, including arylserines, hydroxyaspartic acid, and hydroxyleucine. These bifunctional compounds introduce two chiral centers when used as biomolecular building blocks. Incorporation of unique stereochemistry into the residues of peptide chains can change their properties by, for example, increasing the stability against peptidases and prolonging bioavailability.[9-11] Further, β-hydroxy-α-amino acid scaffolds (Figure 1) are found in clinically important antibiotics, including glycopeptide vancomycin and its analogues, ristocetin from *Amycolatopsis*[12-13] and teicoplanins from *Actinoplanes*,[14] the phenylpropanoid chloramphenicol from *Streptomyces*,[15] and katanosin depsipeptides from *Cytophaga* and *Lysobacter* bacteria.[16-17] The pentapeptide gymnangiamide from marine hydroid *Gymnangium regae* shows anticancer activity.[18] (2*S*,3*R*)-3,4-Dihydroxyphenylserine (DOPS, Droxidopa) is used for hypotension and as a Parkinsonian therapeutic,[19-21] while *N*-arylsulfonyl derivatives of phenylserine ethyl esters function as non-steroidal anti-inflammatory drugs.[22] β-Hydroxy-α-amino acids have also been used recently in protein synthesis by chemical ligation at N-terminal serine and threonine sites, and this technique can likely be expanded to incorporate other non-proteinogenic β-hydroxy amino acids.[23] Additionally, an interesting subclass of non-natural heterocyclic β-hydroxy-α-amino acid amides are drug leads for their analgesic and immunostimulant activities.[24-27]

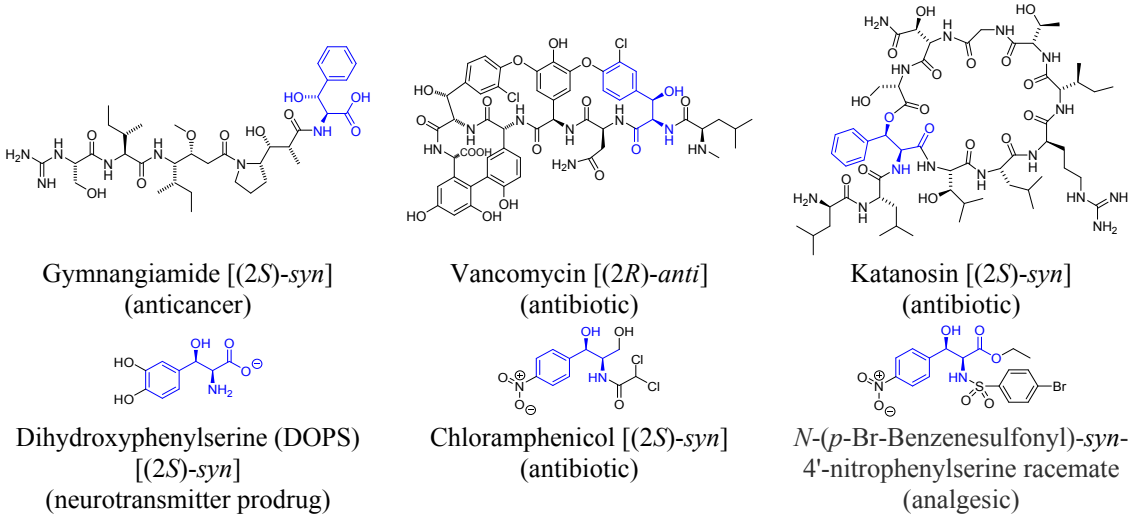

Figure 1. Synthetic and biosynthetic β-phenyl-β-hydroxy-α-amino acid building blocks in bioactive compounds. Stereochemical designations in brackets are described in Figure 2.

Given the beneficial pharmacological, chemical, and physical properties of a compound containing β-hydroxy-α-amino acids, there is considerable interest to make these bifunctional scaffolds by synthetic approaches or combined with biocatalytic routes.[27-29] Various synthetic strategies have been used to control the regio- and stereochemistry of β-hydroxy-α-amino acids, including asymmetric aldol condensation, oxy-Michael addition, electrophilic amination, aminohydroxylation of alkenes, and aza-Claisen rearrangement.[19, 30-33] Several of these methods incorporate protecting group manipulations to direct regiochemistry, add a functionalized chiral auxiliary to incorporate stereogenic centers, or apply heavy-metal catalysts to promote the reactions. These synthetic approaches are often highly efficient and stereoselective, but chemical manufacturers observe that these routes often violate green chemistry principles through generation of heavy-metal waste, poor atom economy built on the synthesis of intricate chiral-ligand catalysts, and frequently fall short as sustainable methods.[34-35]

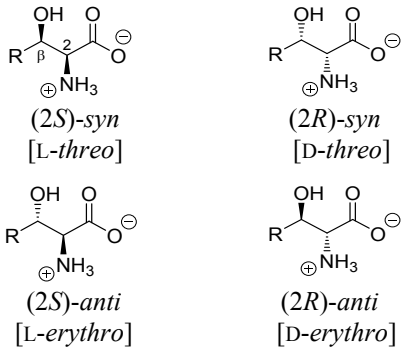

Figure 2. Stereoisomerism convention for β-hydroxy-α-amino acids used herein. The equivalent, archaic designations are listed in brackets.

Biocatalysis is emerging as a valuable complementary tool for organic chemists to access regio- and stereocontrolled chemical transformations that otherwise use complex synthetic chiral ligands and often proceed through multiple steps in conventional methods.[35-38] Biocatalytic routes towards (2*S*)+(2*R*)-(*syn*/*anti*)-β-hydroxy-α-amino acids[39] (Figure 2) mixtures regularly use threonine aldolases (TAs). TAs are divided into two groups depending on the (*R*)- or (*S*)-stereochemistry at the α-carbon of threonine where the amino group is attached. While the substrate specificity of TAs depends on the glycine donor substrate, they have broad specificity for the aldehyde, including non-natural aryl aldehydes when used to produce arylserines.[40] TAs are divided further into four subgroups, depending on the stereochemistry at the β-carbon of threonine, where the hydroxyl group is attached. High-specificity (2*S*)-*syn*-TAs make only (2*S*)-*syn*-threonine analogues, (2*S*)-*anti*-TAs are stereoselective for (2*S*)-*anti*-threonine analogues, while low-specificity (2*S*)-TAs make a mixture of (2*S*)-*syn*- and (2*S*)-*anti*-threonine analogues. Only low-specificity (2*R*)-TAs are known and make mixtures of (2*R*)-*syn*- and (2*R*)-*anti*-threonine analogues.[29]

TA specificity is also used in industrial chemical processes for enantiospecific enzyme resolution to cleave (via a retro-aldol reaction) one enantiomer of a *syn*- or *anti*-β-hydroxy-α-amino acid pair.[29] This process stereospecifically enriches one stereoisomer over the other in a

mixture. For example, a low specificity (2*R*)-TA stereospecifically catalyzed the retro-aldol cleavage of the (2*R*)-isomer in a (2*S*)+(2*R*)-*syn*-racemate to resolve the intact (2*S*)-*syn*-(3',4'-methylenedioxy)phenylserine enantiomer, a precursor of the therapeutic drug (2*S*)-*syn*-DOPS (L-DOPS).[41]

Here, we used an irreversible, TA-*independent* biocatalytic method employing a repurposed 5-methylidene-3,5-dihydro-4*H*-imidazol-4-one (MIO)-dependent phenylalanine aminomutase (*Tc*PAM) from *Taxus canadensis* plants[42-44] to make various ring-substituted phenylserines. In *Taxus* plants, *Tc*PAM isomerizes (2*S*)-α-phenylalanine to (3*R*)-β-phenylalanine on the biosynthetic pathway of the anticancer therapeutic paclitaxel (Taxol®) (Scheme 1).[42-43] The MIO moiety is formed post-translationally by active site residues within *Tc*PAM, and this electrophilic unit transiently becomes N-alkylated by the (2*S*)-α-phenylalanine substrate. The resulting alkyl ammonium group is displaced as an NH_2-MIO adduct with simultaneous removal of H_β.[45] The cinnamate intermediate accepts the amino group from the NH_2-MIO adduct at C_β, and C_α is reprotonated to complete the α- to β-isomerization (Scheme 1).

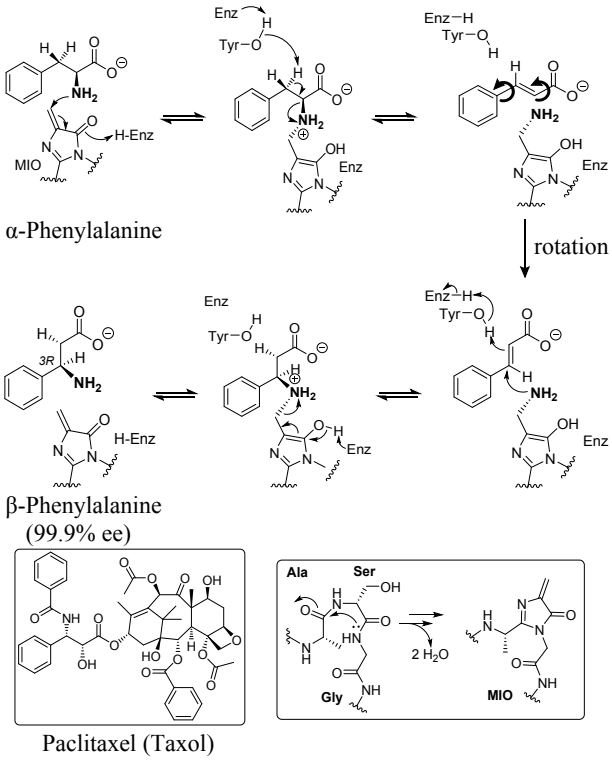

Scheme 1. Mechanism of β-phenylalanine formation catalyzed by *Tc*PAM. *Inset left*: Anticancer drug paclitaxel (Taxol). *Inset right*: Formation of MIO from the condensation of Ala175, Ser176, and Gly177 of *Tc*PAM.

An earlier study covalently trapped a cinnamate epoxide in the active site of an MIO tyrosine aminomutase (*Sg*TAM) crystal to help dissect its enzyme mechanism.[46] The ability of *Sg*TAM to trap an epoxide hinted that the MIO chemistry would be aborted by covalent inhibition. It is interesting to note that the crystal structures of a phenylalanine aminomutase from *Pantoea agglomerans* (*Pa*PAM) in our subsequent study showed dual occupancy of α- and β-phenylalanines (substrate and product, respectively) covalently linked to the MIO moiety through their amino groups.[47] Thus, we reinterpreted the structures of the previous epoxide inhibition study to represent β-hydroxy-α-amino adducts, rather than a dihydroxy ether intermediate attached covalently to the MIO group.[46]

Later, in a burst phase kinetics study, *Tc*PAM was shown to transfer the amino group from a surrogate substrate (2*S*)-styryl-α-alanine to exogenously supplied cinnamates via an NH_2-MIO

adduct.[48] The transaminase function of *Tc*PAM catalyzed efficient intermolecular exchange of the amino group to make a mixture of α- and β-amino acids.[49] Encouraged by the intermolecular mechanism of *Tc*PAM and our reinterpretation of the chemistry of MIO enzymes with epoxides, here, we describe a new application for the catalyst to transfer an amino group to various ring-substituted cinnamate epoxides to make phenylserine analogues. Michaelis-Menten constants of *Tc*PAM catalyzing the epoxide ring-opening chemistry were calculated, and the absolute stereochemistry of each enzymatically derived phenylserine was assessed.

MATERIALS AND METHODS

General Procedure for Syntheses of Cinnamate Epoxides (**2a**–**2l**). The cinnamate epoxides were synthesized according to a procedure described previously.[50] In a 50-mL single-necked round-bottomed flask, a stirred slurry of a *trans*-cinnamic acid analogue (**1a**–**1l**) (0.75 mmol) in acetone (515 μL, 7.5 mmol) was treated first with sodium bicarbonate (3.3 mmol) and then with dropwise addition of water (515 μL). To the resulting thick mixture, a solution of oxone monopersulfate (1.4 mmol, contains 1.8 equiv of $KHSO_5$) in 0.4 mM Na_2EDTA solution (1.6 mL) was added dropwise for 1 h while the temperature was kept at ~25 °C and the pH at 7.5. The mixture was then stirred an additional 6 h and cooled to –5 °C. The reaction was acidified to pH 2 (12 M HCl) and mixed with ethyl acetate (5 mL) with rapid stirring. The mixture was then filtered and extracted with ethyl acetate (3 × 50 mL). The combined organic fractions were washed with saturated NaCl, dried over anhydrous $MgSO_4$, filtered, and concentrated under vacuum. After all the solvent was removed, each *trans*-cinnamic acid epoxide analogue was isolated as an oily residue. The oily residue was dissolved in ethanol (EtOH) (1 mL), cooled on ice, and treated with a solution of KOH (3.6 mmol) dissolved in EtOH (1 mL). The resulting thick slurry was filtered, and the residue was

washed with EtOH and then dried under vacuum to provide the potassium salts of the cinnamate epoxides as a racemic mixture (Table S1, Figures S1 and S2 of the Supporting Information).

Expression and Purification of *Tc*PAM. The *tcpam* cDNA (codon-optimized for expression in bacteria) was ligated into the expression vector pET28a(+),[42] and the recombinant plasmid encoded an N-terminal His_6 tag. *Escherichia coli* BL21(DE3) cells, transformed to express *Tc*PAM, were grown at 37 °C for 12 h in 150 mL of Lysogeny broth (LB). Separate aliquots (25 mL) of this inoculum culture were then added to each of six 1-L cultures of LB supplemented with kanamycin (50 μg/mL). The cells were incubated at 37 °C until OD_{600} = 0.7. Isopropyl-D-thiogalactopyranoside (500 μM) was added to the cultures with expression conducted at 16 °C for 16 h. The cells were harvested by centrifugation at 4,650*g* (15 min), and the pellets were diluted in resuspension buffer (100 mL of 50 mM sodium phosphate containing 5% (v/v) glycerol and 300 mM NaCl, pH 8.0). The cells were then lysed by brief sonication [one 10-s burst at 60% power with a 20-s rest interval for 20 cycles on a Misonix Sonicator (Danbury, CT)]. The cellular debris was removed by centrifugation at 27,200*g* (20 min) followed by high-speed centrifugation at 142,000*g* (90 min) to remove light membrane debris. The resultant crude aminomutase in the soluble fraction was purified by nickel-nitrilotriacetic acid affinity chromatography according to the protocol described by the manufacturer (Invitrogen, Carlsbad, CA); *Tc*PAM eluted in 50 mL of 250 mM imidazole dissolved in resuspension buffer. Fractions containing active soluble *Tc*PAM (76.5 kDa) were combined and loaded onto a size-selective centrifugal filtration unit (30,000 NMWL, Millipore Sigma, Burlington, MA). The protein solution was concentrated and diluted over several cycles until the imidazole and salt concentrations were <1 μM, and the final volume was 1 mL, containing ~14 mg of *Tc*PAM. The quantity of *Tc*PAM was measured using a Nanodrop

spectrophotometer (ThermoFisher Scientific, Waltham, MA) and the purity (82%) was assessed by SDS-PAGE with Coomassie Blue staining using Kodak Gel Logic 100 Imaging System (version 3.6.3) to integrate the relative intensities of the scanned protein bands (Figure S5 of the Supporting Information).

Expression and Purification of (2*S*)-Threonine Aldolase (*ltaE*). A cDNA (from *E. coli*, accession number: P75823) encoding a low specificity (2*S*)-threonine aldolase (*ltaE*) was ligated into a pET28a(+) vector, encoding an appended N-terminal His_6-tag, to make a recombinant plasmid (designated as pKDW014_lsTA) was purchased from GenScript (Piscataway, NJ). *Escherichia coli* BL21(DE3) cells were then transformed with pKDW014_lsTA to overexpress the *ltae* gene by standard protocols (Millipore Sigma, Burlington, MA). Transformed bacteria were used to inoculate LB (100 mL) and grown at 37 °C for 12 h. Separate aliquots (15 mL) of this inoculum culture were added to each of three 1-L cultures of LB supplemented with kanamycin (50 μg/mL). The cells were incubated at 37 °C until OD_{600}= 0.6, and isopropyl-D-thiogalactopyranoside (100 μM) was added to induce expression at 16 °C for 16 h. The cells were harvested by centrifugation at 4,650*g* (15 min), and the pellets were diluted in resuspension buffer (at pH 7.0) containing 10 μM PLP and 300 mM NaCl. The cells were then lysed by brief sonication [one 10-s burst at 60% power with a 20-s rest interval for 20 cycles on a Misonix Sonicator], and the cellular debris was removed by centrifugation at 27,200*g* (20 min) followed by high-speed centrifugation at 142,000*g* (90 min) to remove light membrane debris. The clarified lysate containing crude (2*S*)-TA in the soluble fraction was purified by nickel-nitrilotriacetic acid affinity chromatography according to the protocol described by the manufacturer (Invitrogen, Carlsbad, CA); (2*S*)-TA was eluted in 50 mL of 250 mM imidazole. Fractions containing active soluble (2*S*)-

TA (36.5 kDa) were combined and loaded onto a size-selective centrifugal filtration unit (15,000 NMWL, Millipore Sigma). The protein solution was concentrated and diluted over several cycles until the imidazole and salt concentrations were <1 μM, and the final volume was 1 mL. The concentration of (2*S*)-TA was measured (8.8 mg/mL) using a Nanodrop spectrophotometer (ThermoFisher Scientific). The purity (99%) was assessed by SDS-PAGE with Coomassie Blue staining using Kodak Gel Logic 100 Imaging System (version 3.6.3) to integrate the relative intensities of the scanned protein bands (Figure S5 of the Supporting Information).

Biocatalysis of Phenylserine with *Tc*PAM. A solution of (2*S*)-styryl-α-alanine (1 mM) in 50 mM NaH_2PO_4/Na_2HPO_4 buffer (pH 8.0, 5% glycerol) was preincubated with *Tc*PAM (100 μg/mL) for 2 min. Cinnamate epoxide (1 mM) was added to the solution, and the assay was mixed at 31 °C on a rocking shaker for 2.5 h. The reaction was then stopped with 10% formic acid to adjust the pH to 3.0, and 3'-bromo-α-phenylalanine (50 nM) was added as an internal standard. This reaction mixture was analyzed using a liquid chromatography-electrospray ionization-multiple reaction monitoring (LC/ESI-MRM) method.

Kinetic Analysis. To calculate the steady-state enzyme kinetic constants, each epoxide substrate was varied at intervals from 25 μM up to 1000 μM in triplicate assays containing *Tc*PAM (100 μg/mL). The reactions were terminated with 10% formic acid (pH 3.0) and the resultant ring-opened biocatalyzed products, without derivatization, were quantified by LC/ESI-MRM. The apparent kinetic parameters (K_M and k_{cat}) were calculated by non-linear regression with Origin Pro 9.0 software (Northampton, MA) (Figures S6 and S7 of the Supporting Information), using the

Michaelis-Menten equation: $v_o = [E_o]k_{cat}/(K_M + [S])$. Control assays contained all the necessary components for an operational assay except either the amine group donor (2*S*)-styryl-α-alanine or the enzyme was omitted (Table S3 of the Supporting Information).

General Procedure for the Syntheses of Phenylserines (4a–4l). The phenylserine analogues were synthesized according to a procedure described previously.[51] Triethylamine (22 mmol) was added to a solution of glycine (5 mmol) in water (4 mL). To this solution, a benzaldehyde (10 mmol) analogue was added dropwise over 15 min, and the mixture was stirred for 12 h at ~25 °C. The color of the reaction mixture gradually changed from clear and colorless to yellow-brown. *n*-Butanol (3 mL) was added, and the triethylamine was evaporated under vacuum. The butanolic solution was diluted with water (3 mL), and the mixture was acidified to pH 2 with HCl (6 M). The acidified solution was stirred at ~25 °C for 3 h and partitioned against ethyl acetate (2 × 5 mL) to remove the unreacted benzaldehyde. The aqueous layer was separated and neutralized to pH 6.0 with a saturated $NaHCO_3$ solution to precipitate the phenylserine. The mixture was stirred for 1 h at 0 °C, and the phenylserine product was washed with water (3 mL) and dried under vacuum to yield the corresponding mixture of phenylserine diastereomers.

General Method for Derivatizing Phenylserines with a Chiral Auxiliary. A mixture of all four stereoisomers of phenylserine (0.21 mmol) was dissolved in 50 mM NaH_2PO_4 /Na_2HPO_4 buffer (pH 8.0) containing 5% glycerol (1 mL). To this solution were added pyridine (50 µL, 0.62 mmol) and (*2S*)-2-methylbutyric anhydride (60 µL, 0.30 mmol), and the reaction mixture was stirred for 20 min at ~25 °C. The solution was adjusted to pH 2 (6 M HCl) to quench the reaction, and the *N*-

protected phenylserine was extracted with ethyl acetate (2 mL). The organic layer was separated and evaporated under a stream of nitrogen gas, and the resultant residue was dissolved in 3:1 EtOAc/MeOH (v/v) (1 mL). Diazomethane in diethyl ether was added dropwise to obtain the methyl ester, and the solvent was removed under a stream of nitrogen gas. The resulting methyl ester was dissolved in dichloromethane (1 mL) to which pyridine (100 μL, 1.24 mmol) and chlorotrimethylsilane (150 μL, 1.18 mmol) were added, and the solution was stirred for 15 min at ~25 °C. The reaction was quenched with water (1 mL) and the organic fraction was separated and analyzed by gas chromatography coupled with electron-impact mass spectrometry (GC/EI-MS).

RESULTS AND DISUSSION

Synthesis of Racemic Epoxide Substrates. Various commercially available cinnamic acids (**1a**–**1l**) were oxidized with Murray's reagent to synthesize the corresponding ring substituted cinnamate epoxides (**2a**–**2l**) as their racemates (see Scheme 2, entry **4** for assignment of substituents **a**–**l**).[50] The enantiomeric ratios of each racemate methyl ester was ~1:1 by chiral GC/EI-MS analysis (Figures S1 and S2 of the Supporting Information). Trifluoroacetone was used instead of acetone to modify Murray's reagent and oxidize the less reactive NO_2-cinnamate analogues to epoxides **2g** and **2h**. The 4'-OCH_3-cinnamate epoxide rapidly hydrolyzed to the dihydroxy compound under these reaction conditions and thus could not be tested in this study.

Biocatalysis of Arylserines. Each epoxide was incubated separately with the previously employed amine donor (2*S*)-styryl-α-alanine (**3**) and the mutase[48] at pH 8.0 to make the phenylserines. (2*S*)-Styryl-α-alanine (**3**) was the amine donor that loaded an NH_2 group on the MIO moiety of *Tc*PAM instead of 6 M ammonium salts at pH 9 used in several previous studies to convert various cinnamates to α- and β-amino acids.[44, 52-53] Another synthesis study informed

that high concentrations of ammonia could non-enzymatically aminate cinnamate epoxide nearly exclusively at the benzylic carbon (C_β), converting it to phenylisoserine.[54] This selective amination of cinnamate epoxide at C_β is directed by the ability of the benzylic carbon to resonance stabilize the δ^+ formed in the transition state. This electronic-based regioselectivity would therefore be sensitive to the electronic effects of substituents on the aryl ring. Control experiments (with or without the *Tc*PAM catalyst) in this study showed that after incubating 2 M NH_3 (NH_4OH in 50 mM phosphate buffer, pH 8) for 2.5 h with the cinnamate epoxide bearing a mesomerically electron-withdrawing 4'-NO_2 (**2h**), the amination reaction yielded a ~40:60 mixture of isoserine to serine, with the latter predominating (Figure S3 of the Supporting Information). The 4'-NO_2 group ($\sigma_{4'\text{-}NO_2}$ = 0.78) (where σ is the Hammett substituent constant)[55] is positioned to pull electron density of the epoxide oxygen toward C_β, polarize the C_α–O bond, and thus encourage nucleophilic amination at C_α to form mostly phenylserines as observed. By contrast, cinnamate epoxide (**2a**) ($\sigma_{[H]}$ = 0.0) and its 3'-OCH_3 (**2b**) ($\sigma_{[3'\text{-}OCH_3]}$ = 0.12) and 4'-CH_3 (**2i**) ($\sigma_{[4'\text{-}CH_3]}$ = -0.17) analogues have similar electronic influence on the epoxide ring opening. Substrates **2a**, **2b**, and **2i** favored intrinsic amination at C_β to form the arylisoserines at ≥93% compared to the lesser amount of serine when incubated with 2 M NH_3 (Figure S3), as observed in earlier synthetic studies.[54, 56] Thus, (2*S*)-styryl-α-alanine (**3**) was chosen as a milder amine source to dissect the regiochemistry and stereoselectivity of *Tc*PAM transamination catalysis.

Assessing the Regiochemistry of the TcPAM-catalyzed Transamination Reaction. The regiochemistry and relative stereochemistry of the mutase amination reaction were assigned by derivatizing the products made from enzyme catalysis. For example, authentic racemic (2*S*)+(2*R*)-*syn*-phenylserine [(2*S*)+(2*R*)-*syn*-**4a**] and (2*R*,3*S*)-*syn*-phenylisoserine [(2*R*,3*S*)-*syn*-**4a**] standards (Scheme 2 insets) were converted to their *O*-trimethylsilyl *N*-[(2*S*)-2-methylbutyryl] methyl esters

(Scheme 2A). The diagnostic fragment ions in the GC/EI-MS profile for the derivatized authentic phenylserine racemate were identical to those of the enzymatically derived phenylserine diastereomers yet distinct from those of the (2*R*,3*S*)-*syn*-phenylisoserine ((2*R*,3*S*)-*syn*-**5a**) standard derivatized identically (Figure 3). GC/EI-MS fragmentation of the other biocatalytically made phenylserine analogues (**5a**–**5l**) was identical to the ion profiles of the corresponding synthetic phenylserine analogues derivatized identically (Scheme 2B and Figures S8–S18 of the Supporting Information).

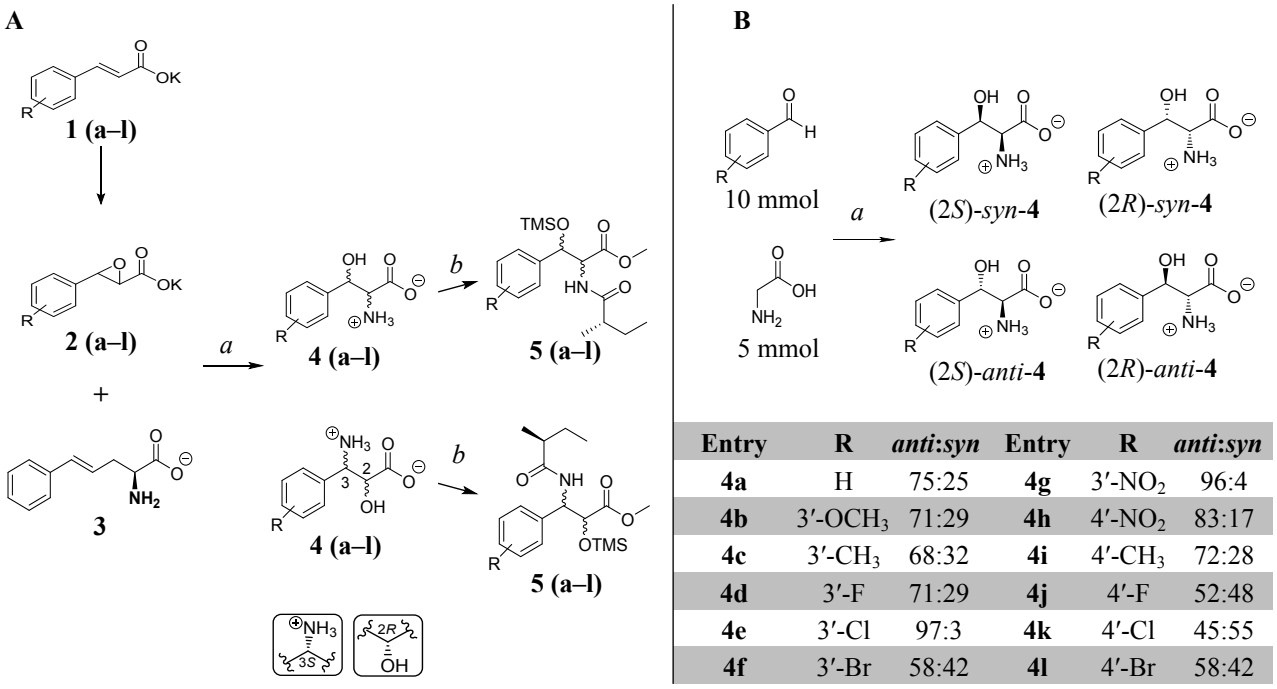

Entry	R	*anti*:*syn*	Entry	R	*anti*:*syn*
4a	H	75:25	**4g**	3′-NO_2	96:4
4b	3′-OCH_3	71:29	**4h**	4′-NO_2	83:17
4c	3′-CH_3	68:32	**4i**	4′-CH_3	72:28
4d	3′-F	71:29	**4j**	4′-F	52:48
4e	3′-Cl	97:3	**4k**	4′-Cl	45:55
4f	3′-Br	58:42	**4l**	4′-Br	58:42

Scheme 2. A) *Tc*PAM was incubated with (2*S*)-styryl-α-alanine (**3**) (1 mM) and separately with each *trans*-cinnamate epoxide racemate **2a**–**2l** made from cinnamic acids **1a**–**1l**. Step *a*) *i*) *Tc*PAM (1.7 mg/mL) in 50 mM NaH_2PO_4/Na_2HPO_4 (pH 8.0), 5% glycerol, 2 min pre-equilibration, **2a**–**2l** (10 mM), 29 °C, 4 h. Step *b*) Derivatization of putative phenylserines and phenylisoserines using a chiral auxiliary for stereoisomeric resolution. *i*) (2*S*)-2-Methylbutyric anhydride, pyridine, rt, 20 min; *ii*) 6 M HCl, pH 2; *iii*) CH_2N_2, EtOAc/MeOH (3:1 *v*/*v*), rt, 15 min; and *iv*) chlorotrimethylsilane, pyridine, CH_2Cl_2, rt, 15 min. *Insets*: stereoisomerism of (2*R*,3*S*)-*syn*-phenylisoserine. B) Synthesis of the stereoisomers of phenylserine analogues from glycine and a substituted benzaldehyde. a) step *i*) triethylamine, *n*-BuOH and H_2O, 12 h, rt; step *ii*) 6 M HCl, pH 2; and step *iii*) $NaHCO_3$, pH 6.

*Tc*PAM could theoretically transfer the amino group to either C_α or C_β of the oxirane substrate to make phenylserine or phenylisoserine, respectively. We hypothesized that the aryl ring alone and the electronics of the substituents attached to it would differentially affect the reactivity at C_β

toward nucleophilic amination, as they did in our control experiments. However, the regiochemical analysis showed that regardless of the electronic nature of the substituent attached to the aryl ring, *Tc*PAM aminated predominantly at C_α to open the cinnamate epoxides.

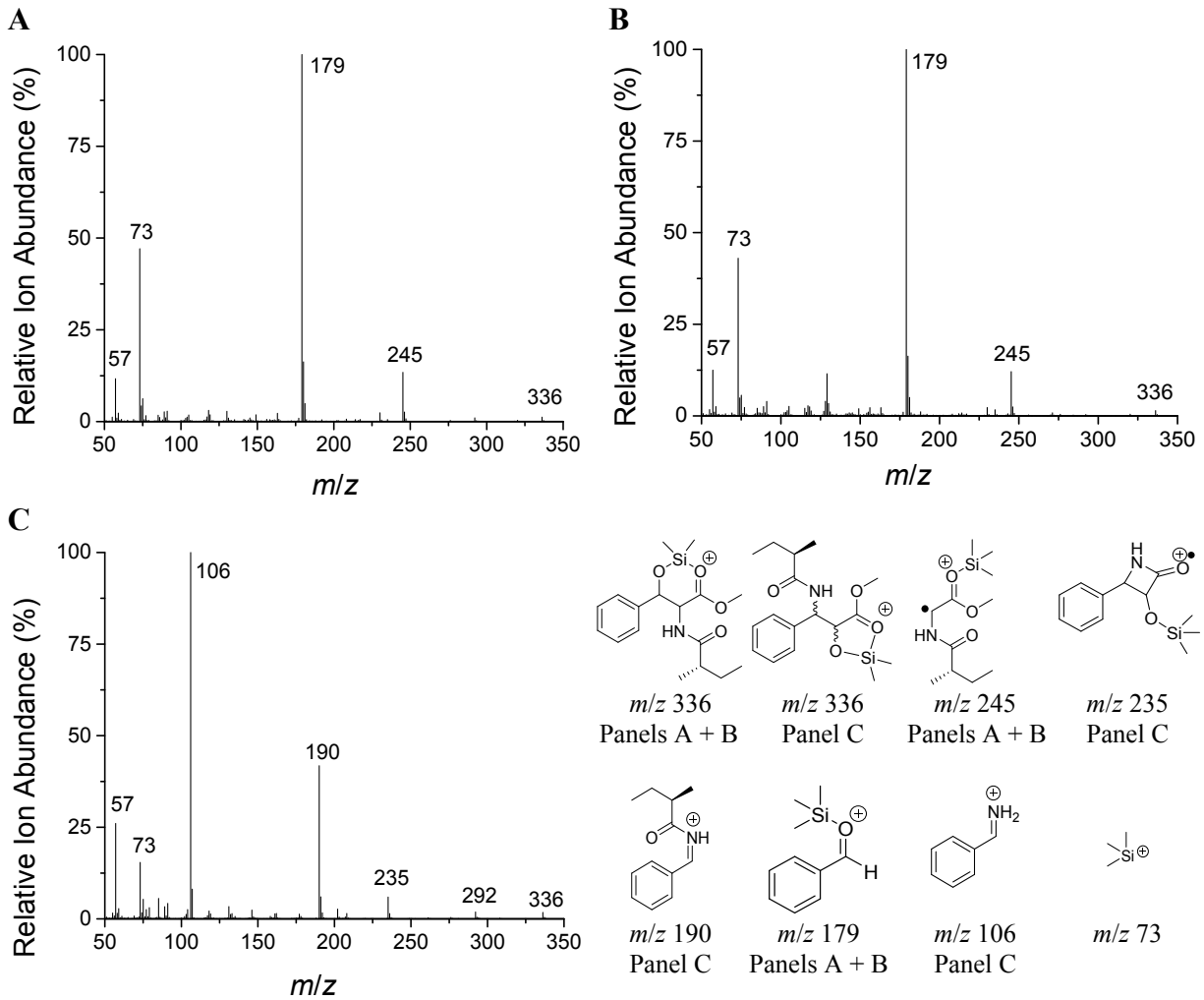

Figure 3. GC/EI-MS spectra of authentic A) (2*S*)+(2*R*)-*syn*-phenylserine from Sigma-Aldrich, B) phenylserine biocatalyzed from cinnamate epoxide by *Tc*PAM catalysis (see Figure 5 for GC profiles), and of C) (2*R*,3*S*)-*syn*-phenylisoserine (see Figure S4 of the Supporting Information for GC profile). Each hydroxyamino acid was derivatized to its *O*-trimethylsilyl *N*-[(2*S*)-2-methylbutyryl] methyl ester. The molecular ion (M•+, *m/z* 351) was not observed for either analyte.

Relative Stereochemistry of TcPAM reaction by ^{1}H NMR Analysis. A ^{1}H NMR method was used to establish the relative *syn*/*anti*-stereochemistries of the four synthesized arylserine diastereomers. The coupling constants for the vicinal protons (H_α and H_β) were similar ($^3J_{H_\alpha\text{-}H_{\beta(anti)}}$ and $^3J_{H_\alpha\text{-}H_{\beta(syn)}} \approx 4$ Hz) for the underivatized synthetic *anti*- and *syn*-phenylserine diastereomers.

Thus, differences in H_α and H_β coupling constants could not be used to distinguish the *anti*- and *syn*-diastereomers, as done in another study.[57] Thus, a small amount of authentic (2*S*)+(2*R*))-*syn*-phenylserine racemate was added to the synthesized mixture of *anti*- and *syn*-phenylserine diastereomers (Figure 4A). The ^{1}H NMR of the "spiked" sample showed a relative increase of the doublet pair ("outer doublets") at δ 4.23 and δ 5.41 (Figure 4B). The chemical shift difference (Δδ) of 1.15 ppm at pH 1.5 for the "outer doublets" assigned these signals to the *syn*-phenylserine enantiomers. The "inner doublets" at δ 4.33 and δ 5.37 ($\Delta\delta_{anti}$ = 1.04 ppm, pH 1.5) were thus assigned to the *anti*-phenylserine enantiomers. We used the trends in the Δδ values to assign the relative *anti*/*syn*-stereochemistries and *anti*:*syn* ratios of the remaining synthetic and bicatalytically derived phenylserine analogues without derivatization (Table 1).

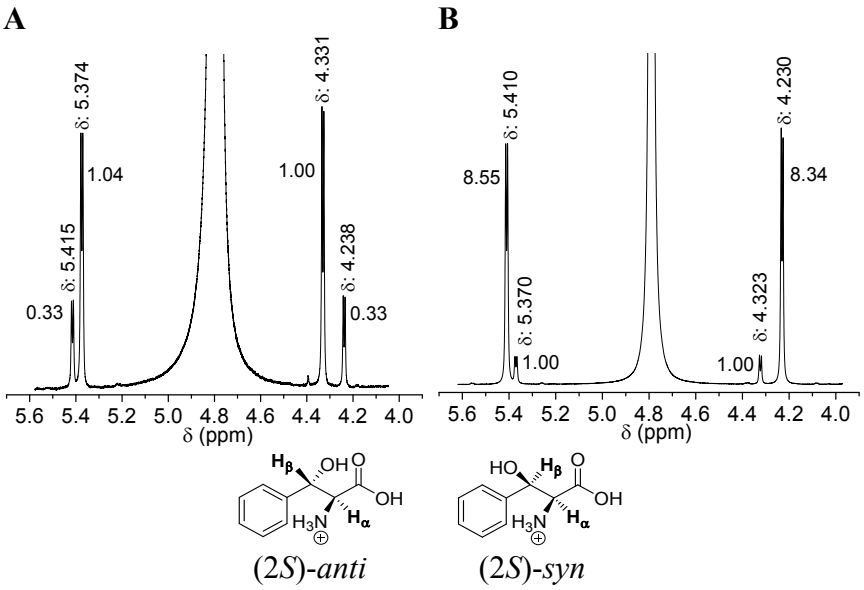

Figure 4. An expanded 500 MHz ^{1}H NMR of A) synthesized phenylserine (**4a**), and B) of **4a** containing authentic (*2S*)-*syn*-phenylserine (see Figure 2) recorded in D_2O at pH 1.5. Chemical shift values are listed vertically above each peak, and the relative area under each peak is listed horizontally next to each peak.

Each chemically and enzymatically synthesized arylserine analogue was dissolved separately in D_2O at pH 1.5 and analyzed by ^{1}H NMR. The $\Delta\delta_{syn}$ (~1.15 ppm, pH 1.5) of the "outer doublets" was consistently larger than the ($\Delta\delta_{anti}$) (~1.05 ppm, pH 1.5) for the "inner doublets" (Figures S19–

S30 of the Supporting Information). The NMR analysis substantiated that *Tc*PAM aminated the epoxide substrates predominantly at C_α to produce *anti*-arylserine analogues as the major product, regardless of the substituent on the aryl ring. A smaller amount (≤9%) of the *syn*-phenylserines was also made.

Table 1. 500 MHz ^{1}H NMR Data for Synthetically and Biocatalytically Produced Phenylserine Analogues (**4a**–**4l**).

	R	$^3J_{H_\alpha\text{-}H_\beta}$ *anti* (Hz)	$^3J_{H_\alpha\text{-}H_\beta}$ *syn* (Hz)	$\Delta\delta_{anti}$[b] (ppm)	$\Delta\delta_{syn}$[b] (ppm)	$^3J_{H_\alpha\text{–}H_\beta}$ biocatalyzed (Hz)	$\Delta\delta_{biocatalytic}$ (ppm)	*anti*:*syn*[c] (NMR)[a]	*anti*:*syn*[c] (GC-MS)
4a	H	4.0	4.0	**1.04**	1.17	4.0	**1.05**	93:7	91:9
4b	3′-OCH_3	4.0	4.0	**1.02**	1.15	4.0	**1.02**	100:0	95:5
4c	3′-CH_3	4.0	4.0	**1.00**	1.14	4.0	**1.01**	100:0	96:4
4d	3′-F	4.0	4.0	**1.02**	1.16	4.0	**1.04**	98:2	95:5
4e	3′-Cl	4.0	4.0	**1.03**	1.18	4.0	**1.01**	91:9	94:6
4f	3′-Br	4.0	4.0	**1.02**	1.17	4.0	**1.02**	93:7	92:8
4g	3′-NO_2	4.0	4.0	**1.08**	1.21	3.5	**1.08**	93:7	92:8
4h	4′-NO_2	3.5	4.0	**1.06**	1.22	4.0	**1.09**	97:3	96:4
4i	4′-CH_3	4.0	4.0	**1.00**	1.13	4.0	**0.99**	100:0	95:5
4j	4′-F	4.0	4.0	**1.03**	1.16	4.0	**1.03**	93:7	97:3
4k	4′-Cl	4.0	4.0	**1.03**	1.16	4.0	**1.00**	100:0	91:9
4l	4′-Br	4.0	4.0	**1.00**	1.13	4.0	**0.98**	100:0	95:5

[a]"0" indicates that the *syn*-isomer was below the limits of detection of the NMR (at ~100 nmol). [b]$\Delta\delta_{anti}$ and $\Delta\delta_{syn}$ values for the synthetic phenylserine analogues. [c]*anti*:*syn* ratio for the biocatalytically produced phenylserine analogues. n = 3. Standard error < 1%.

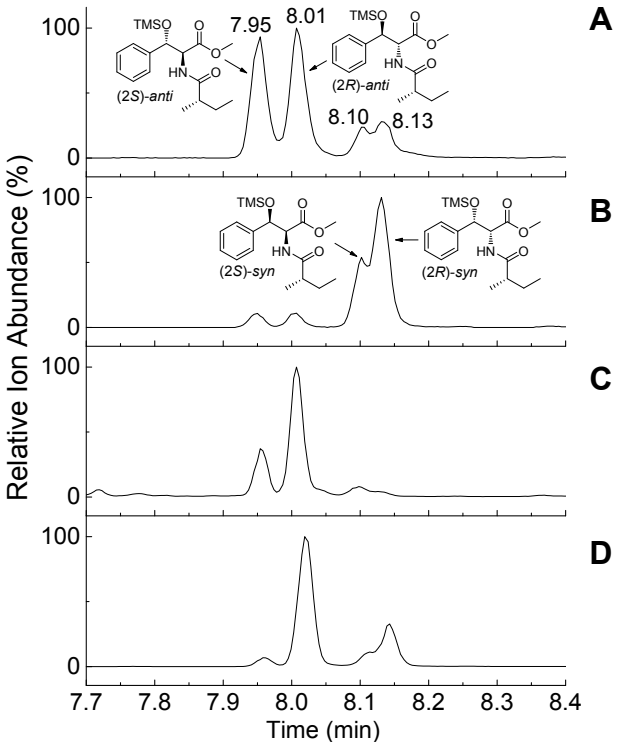

Figure 5. Gas-chromatography/mass spectrometry extracted-ion chromatograms with *m*/*z* 179 ion monitoring of A) synthesized phenylserine as shown in Scheme 2B was derivatized with a chiral auxiliary as per Scheme 2A. Peaks at 7.95 min and 8.01 min correspond to (2*S*)+(2*R*)-*anti*-phenylserine isomers, and those at 8.10 and 8.13 min correspond to (2*S*)+(2*R*)-*syn*-phenylserine isomers; B) derivatized authentic (2*S*)+(2*R*)-*syn*-phenylserine racemate (Sigma-Aldrich, contains 13% (2*S*)+(2*R*)-*anti*-phenylserine as an impurity; C) chiral-auxiliary of biocatalyzed phenylserine made from the cinnamate epoxide racemate. Biocatalyzed (2*S*)+(2*R*)-*syn*-phenylserine stereoisomers were also produced at ~9% (peaks at 8.10 and 8.13 min); and D) Extracted ion (*m*/*z* 179) chromatogram of derivatized phenylserine after treating with (2*S*)-TA for 15 min.

Relative Stereochemistry of the TcPAM Reaction by Chiral Auxiliary Derivatization. An orthogonal GC/MS separation method was used to verify the relative stereochemistry of the biocatalyzed arylserines assigned earlier in this study by a ^{1}H NMR method. The chiral *N*-(*S*)-methylbutyryl-*O*-trimethylsilyl methyl ester derivatization of the arylserines described herein were extended to a diastereomeric mixture of synthesized (2*S*)+(2*R*)-*syn*-**4a** and (2*S*)+(2*R*)-*anti*-**4a** (Figure 5A), commercial grade (2*S*)+(2*R*)-*syn*-**4a** (Figure 5B), and **4a** biocatalyzed by *Tc*PAM

from the cinnamate epoxide racemate (**2a**) (Figure 5C) (Scheme 2A). GC/MS profiles for the *N*,*O*-derivatives of the commercial (2*S*)+(2*R*)-*syn*-phenylserine had major peaks at retention times 8.10 min and 8.13 min (Figure 5B) and thus established the stereochemistry of the later-eluting isomeric pair in the mixture. The retention times of these most abundant peaks in the commercial sample matched those of the lower abundant peaks for the derivatized isomers in the synthetic **4a** sample (Figure 5A). The derivatized enantiomers in the phenylserine diastereomeric mixtures eluting at 7.95 min and 8.01 min were therefore assigned as (2*S*)+(2*R*)-*anti*-phenylserine (Figure 5).

In summary, the derivatives of the *anti*-phenylserine enantiomers eluted first, and the *syn*-phenylserine enantiomers eluted later from the GC/MS. In the biocatalyzed sample, *Tc*PAM diastereoselectively turned over the racemate of cinnamate epoxide to a mixture of (2*R*)+(2*S*)-*anti*-phenylserines with one enantiomer predominating (Figure 5C). The arylserines made from epoxides **2b**–**2l** by *Tc*PAM catalysis were derivatized to **5b**–**5l** and analyzed by GC/MS to assign the relative stereochemistries (Figures S31–S33). The biocatalyzed products contained (2*R*)+(2*S*)-*anti*-arylserines as the major stereoisomers, with one enantiomer predominating, while the (2*R*)+(2*S*)-*syn*-arylserines were minor, at ≤9% relative abundance (Table 1).

Absolute Stereochemistry of the TcPAM Reaction by Aldolase Resolution. To assess which enantiomer was biocatalyzed more abundantly among the (2*R*)+(2*S*)-*anti*-arylserines, we used a low specificity (2*S*)-threonine aldolase (TA) from *E. coli*.[58] This enzyme resolution step cleaved the (2*S*)-*anti* diastereomers into a benzaldehyde moiety and glycine, resolving the synthesized (2*R*)-*anti* hydroxy amino acid diastereomers. Each stereoisomeric mixture of synthesized arylserine (entries **4a**–**4l**) was treated with (2*S*)-TA. Aliquots were withdrawn at 15 min under steady-state enzymatic turnover to measure the relative abundances of the arylserine

diastereomers. The remaining arylserine stereoisomers were treated sequentially with (2*S*)-2-methylbutyric anhydride, diazomethane, and chlorotrimethylsilane.

GC/EI-MS analysis of each derivatized arylserine showed that the peak corresponding to the (2*S*)-*anti* isomer diminished relative to that for the (2*R*)-enantiomer (see Figure 5D and Figures S46–S49 of the Supporting Information). We could then assign the 2*R*-*anti* and 2*S*-*anti*-isomers of each arylserine and calculate the 2*R*:2*S*-*anti* ratios of the biocatalyzed arylserines (Figure 6). The 2*R*:2*S*-*anti* ratios for the biocatalyzed arylserines ranged from 66:34 (4'-fluorophenylserine, **4j**) to 88:12 (3'-nitrophenylserine, **4g**) with the (2*R*)-*anti* isomer predominating (Figure 6 and Figures S31–S33 of the Supporting Information). The 2*R*:2*S* ratios for each biocatalyzed *syn*-product could not be calculated accurately because of their ~10-fold lower abundance than the *anti*-isomers and poorer resolution on the GC/MS (see Figure 5B as an example). The *anti*:*syn* ratios calculated from the abundance of derivatized biocatalyzed phenylserines determined by GC/MS analysis agreed with those calculated by the ^{1}H NMR method for the underivatized biocatalytically made arylserines (Table 1). No clear trend explained how a combination of substituent electronic effects, position, and sterics influenced the *R*:*S* ratios of the isoserines made.

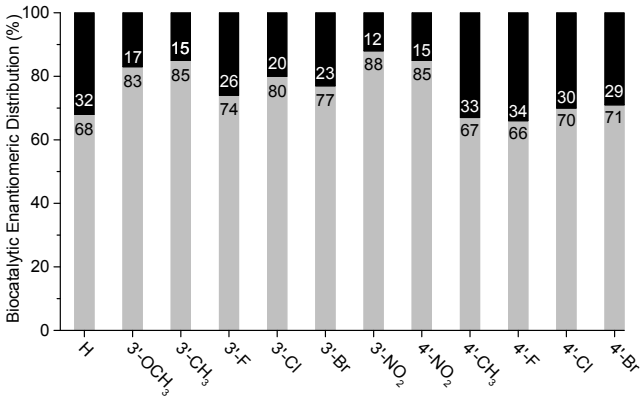

Figure 6. Distribution of enantiomers (2*R*)-*anti* (gray bars) and (2*S*)-*anti* (black bars) in biocatalyzed products for the substituted phenylserine analogues.

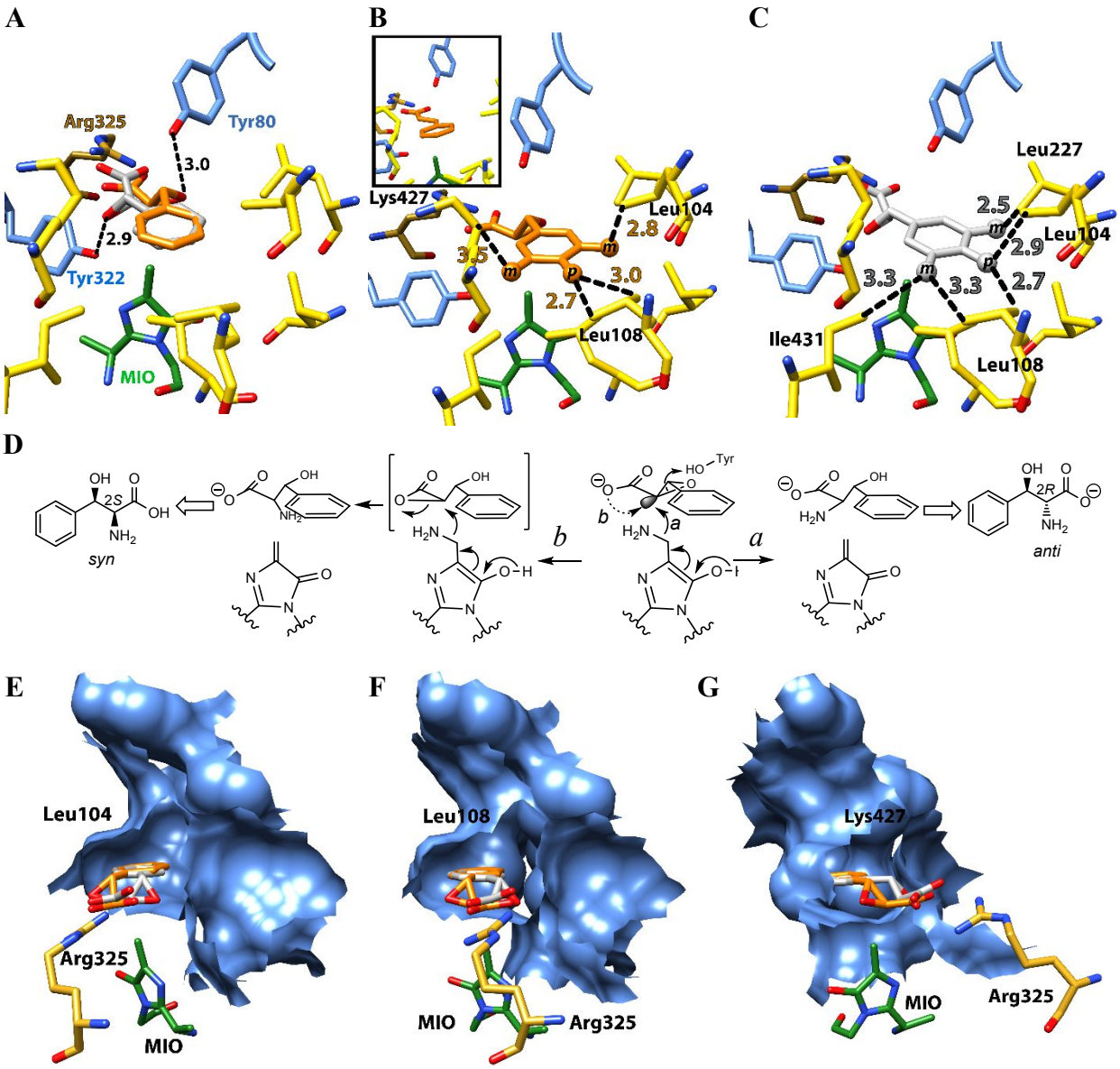

Figure 7. A) Low-energy binding poses are shown of (2*S*,3*R*)-cinnamate epoxide ((2*S*,3*R*)-**2a**) (orange sticks) and (2*R*,3*S*)-cinnamate epoxide ((2*R*,3*S*)-**2a**) (light-gray sticks) at center of the image. The conformations are consistent with the active site of *Tc*PAM consisting of residues (shown as yellow sticks), the catalytic Tyr80, a putative catalytic Tyr322 (light blue sticks), binding contact Arg325 (golden-rod sticks), and the methylidene imidazolone (MIO) moiety (green sticks). B) (2*S*,3*R*)-**2a** (orange sticks) and C) (2*R*,3*S*)-**2a** (light-gray sticks) are posed separately in the active site to highlight the nominal distances (<3.5 Å) that substituents on the aryl ring are from active site residues. Inset) *Tc*PAM in complex with cinnamic acid, based on PDB codes 3NZ4 and 4CQ5. Printed on the aryl ring, '*m*' designates *meta*-positions (equivalent to the 3'-designation used in the text) and '*p*' designates the *para*-position (equivalent to the 4'-designation used in the text) per ligand. Heteroatoms are colored red for oxygen and blue for nitrogen. The images were produced with UCSF Chimera,[59] and the docking conformations were generated with AutoDock Vina[60] from PDB code 3NZ4. Numbers are distances in Å. D) *a*) Rendering of the mechanism showing attack of the NH_2-MIO on the σ* antibonding orbital (gray lobe) at C_α for the C–O σ bond of (2*S*,3*R*)-**2a** to produce (2*R*)-*anti*-phenylserine. *b*) A double inversion-of-configuration mechanism is envisioned to access the minor *syn*-stereoisomer that proceeds through a putative lactone intermediate. Various viewing angles centering on the surfaces of E) Leu104, F) Leu108, and G) Lys427 deep in the aryl binding pocket of *Tc*PAM (PDB code 3NZ4) with poses of the docked (2*S*,3*R*)-**2a** (orange sticks) and (2*R*,3*S*)-**2a** (light-gray sticks).

Epoxide Substrate Docking Model of TcPAM. We used solved structures of *Tc*PAM in complex with cinnamic acid (PDB: 3NZ4 and 4CQ5)[45, 52] (Figure 7B, *inset*) to help interpret whether the proposed dockings of cinnamate epoxides in the *Tc*PAM active site by the AutoDock program were reasonable. The cinnamate epoxides (2*S*,3*R*)-**2a** and (2*R*,3*S*)-**2a** docked in the crystal structure of the *Tc*PAM active site (Figure 7A, B, and C) were consistent with the conformation of the naturally occurring cinnamate intermediate in the crystal structure (Figure 7B, *inset*); the carboxylate group pointed toward Arg325, and the aryl binding region comprised key residues Ile431, Leu108, Leu104, and Leu227 (Figure 7B and C). The docking information suggested that (2*S*,3*R*)-**2a** yields the (2*R*)-*anti*-phenylserine (Figure 7D). The *anti*-stereochemistry of the arylserine products follows a mechanism proceeding through backside nucleophilic attack (S_N2) by the NH_2 group at C_α of the epoxide ring. The docked conformation of (2*S*,3*R*)-**2a** places the epoxide oxygen 3.0 Å from the catalytic Tyr80 of *Tc*PAM. Tyr80 normally functions as a general acid/base during the natural α- to β-phenylalanine isomerase reaction catalyzed by *Tc*PAM. Here, we believe Tyr80 also serves as a general acid to promote protonation-initiated epoxide opening during amination by the NH_2-MIO. Conversely, the docked (2*R*,3*S*)-**2a** enantiomer is poised for making the (2*S*)-*anti*-isomer. The oxirane oxygen of (2*R*,3*S*)-**2a** sits 2.9 Å from Tyr322 that has been identified as a key residue involved in forming the MIO moiety and keeping the NH_2-MIO adduct deprotonated so that it functions as a nucleophile during the normal *Tc*PAM-catalyzed isomerase reaction (Figure 7A).[61] *Tc*PAM likely uses Tyr322 effectively as a surrogate general acid for protonation-initiated epoxide opening during amination by the NH_2-MIO of (2*R*,3*S*)-**2a**.

In this study, the *syn*-stereoisomers for each epoxide were made at low levels compared to the *anti*-isomers, and their resolution as chiral derivatives on GC/MS was poor; thus accurate measurements of the ratio of the *syn*-enantiomers could not be made. The (2*S*)- and (2*R*)-*anti*-

arylserine isomers are made through S_N2 attack by the amino group on the σ* antibonding orbital of C_α–O bond of the (2*S*,3*R*)- and (2*R*,3*S*)-epoxide racemates (Figure 7D, route *a*). However, the 2*S*- and 2*R*-*syn*-arylserine diastereomers cannot be accessed through a similar S_N2-type mechanism unless *Tc*PAM can rotate the substrate into a cisoid conformation that aligns C_α in a proper orientation for nucleophilic attack.

Earlier mechanistic studies suggest that during its natural reaction, *Tc*PAM rotates the cinnamate intermediate about a central axis through a bicycle-pedal motion to invert the faces of the α- and β-carbons 180° from their original positions.[45, 61] This rotation enables the NH_2 group of the MIO adduct to add to the opposite face of C_β from which it was removed from the phenylalanine substrate (see Scheme 1). The oxirane ring prevents rotations about the axis between C_α and C_β. Thus, a double inversion-of-configuration mechanism is envisioned to access the minor *syn*-stereoisomers (<10% relative abundance) that proceeds through a putative lactone intermediate (Figure 7D, route *b*).[62] Through the proposed lactone intermediate pathway, the (2*S*,3*R*)-cinnamate epoxide that produces the more abundant (2*R*)-*anti*-phenylserine at 8.01 min (Figure 5C) likely also makes the 2*S*-*syn* serine isomer (Figure 7D) (see peak at 8.10 min), and the (2*R*)-*syn* isomer at 8.13 min (Figure 5C) is likely derived from the (2*R*,3*S*)-cinnamate epoxide. The other ring-substituted epoxides behaved similarly (Figures S31–S33).

Kinetics of Serine Biocatalysis. The Michaelis parameters were measured by quantifying the underivatized biocatalyzed products by LC/MS-MRM analysis. The apparent K_M and k_{cat} of *Tc*PAM were calculated under steady-state conditions for the analogues of cinnamate epoxide with the amino donor (**3**) at 1 mM (Table 2 and see Figure S50 of the Supporting Information showing the conversion of four example epoxides at 400 μM over 6 h). The catalytic efficiency (k_{cat}/K_M) of *Tc*PAM for 3'-CH_3-cinnamate epoxide (**2c**) was the best among all substrates tested; largely

influenced by its relatively lower K_M compared to those for the 3'-halo (**2d**, **2e**, and **2f**), 3'-NO_2 (**2g**), 4'-NO_2 (**2h**), and 4'-CH_3 (**2i**) substrates. In addition, the catalytic efficiencies of *Tc*PAM for **2c** and two other 3'-substituted cinnamate epoxides (3'-F (**2d**) and 3'-Cl (**2e**)) were superior to those of their 4'-substituted counterparts; k_{cat}/K_M values for the latter two were principally influenced by their higher k_{cat} compared to those of their 4'-substituted isomers (**2j** and **2k**).

We note that *Tc*PAM catalyzes its natural α- to β-amino acid isomerization reaction at 3.0 min^{-1},[45] which is ~10-fold faster than the average turnover rate (~0.3 min^{-1}) of *Tc*PAM for the 3'-substituted cinnamate epoxide substrates used in this study. However, the latter rate is similar to the average rate at which other MIO-dependent aminomutases catalyze their natural α- to β-amino acid isomerization reactions involved in specialized metabolism.[63] Thus, the turnover of the 3'-substituted cinnamate epoxides by *Tc*PAM is within the same order of magnitude as mutases that make β-amino acids in their natural hosts to confer an evolutionary advantage.

Since the calculated docking conformations of the cinnamate epoxides agreed with those of other MIO-enzymes in complex with their natural phenylpropanoid substrates,[45-47, 52] we therefore used the models to help interpret how the position of the substituents could potentially affect catalysis due to steric interactions. Substrate docking models show that for each ligand enantiomer one of the two 3'- ("*meta*"-) carbons of the aryl ring of the substrate can position its substituent in steric relief when pointed toward Lys427 (Figure 7B) and Ile431 (Figure 7C and G). This in part suggests that substrates **2c**, **2d**, and **2e** with relatively smaller 3'-substituents (CH_3, F, and Cl, respectively) are more able to adopt a catalytically competent conformation compared to their 4'-isomers. The latter place substituents on the 4'- ("*para*"-) carbon of each ligand in greater steric conflict with Leu104 (Figure 7B), Leu108, and Leu227 (Figure 7C, E, and F), likely preventing epoxides **2i**, **2j**, and **2k** from being turned over as efficiently (Table 2) (Figures S51 and S52).

Table 2. Kinetics of *Tc*PAM for Turnover of Epoxides (**2a–2l)** to Serines (**4a–4l**) and Isoserines (**4a–4l**).

Entry	R	k_{cat}^{Ser} (min^{-1})	k_{cat}^{Iso} (min^{-1})	K_M (μM)	k_{cat}/K_M (M^{-1} s^{-1})	Entry	R	k_{cat}^{Ser} (min^{-1})	k_{cat}^{Iso} (min^{-1})	K_M (μM)	k_{cat}/K_M (M^{-1} s^{-1})
2a	H	0.39 (0.10)[a]	0.003 (<0.001)	340	19	**2g**	3'-NO_2	0.43 (0.07)	0.01 (0.001)	760	10
2b	3′-OCH_3	0.46 (0.14)	0.27 (0.15)	2000	6.5	**2h**	4'-NO_2	0.75 (0.11)	0.004 (<0.001)	610	21
2c	3′-CH_3	0.31 (0.01)	0.03 (0.001)	50	113	**2i**	4′-CH_3	0.17 (0.03)	0.11 (0.01)	450	10
2d	3'-F	0.62 (0.03)	0.009 (<0.001)	170	61	**2j**	4'-F	0.04 (<0.01)	0.005 (<0.001)	40	17
2e	3'-Cl	1.3 (0.1)	0.10 (0.01)	600	41	**2k**	4'-Cl	0.01 (<0.01)	0.002 (<0.001)	50	4.5
2f	3'-Br	0.02 (<0.01)	0.002 (<0.001)	140	2.5	**2l**	4'-Br	~0.04 (<0.01)	0.01 (<0.001)	50	15

[a]Standard deviation in parenthesis (n = 3). The "<" symbol indicates that the actual value, estimated to one significant figure, is shown. k_{cat}^{Ser} is the apparent k_{cat} of arylserine production, k_{cat}^{Iso} is the apparent k_{cat} of arylisoserine production, and k_{cat} is the turnover rate for the production of both arylserine and arylisoserine by *Tc*PAM. The K_M of *Tc*PAM for each substrate is calculated from the production of arylserine and arylisoserine combined.

Furthermore, the 3'-Cl-cinnamate epoxide (**2e**) was turned over (k_{cat}) by *Tc*PAM faster than the other epoxides in this study and interestingly much more superior (>130-fold) than the 4'-Cl isomer (**2k**) (Table 2). The other 3'-substituted analogues turned over ~16-fold and ~2-fold faster than their 4'-substituted counterparts (**2j** and **2i**) were the 3'-F- (**2d**) and 3'-CH_3- (**2c**) cinnamate epoxides, respectively. The larger steric 3'-Br- (**2f**) and 4'-Br- (**2l**) substrates were turned over with poorer catalytic efficiency, due mainly to their equally poor k_{cat} values. The K_M values of *Tc*PAM for both Br-substituted substrates were similar yet lower (estimating tighter binding) than for other substrates such as **2d**, **2e**, **2g**, and **2h** that were turned over faster (Table 2). This suggests that a yet unknown phenomena resulting in part from tighter binding and steric misalignment likely disrupted the turnover of the bulkier bromo-substituted substrates by *Tc*PAM (Figure S51A and B, and Figure S52A and B of the Supporting Information).

It was interesting to find that the 3'-OCH_3-cinnamate epoxide (**2b**) with the largest estimated steric volume[64-65] (26.4 Å^3) was turned over similar to most 3'-substituted substrates with smaller substituents, such as H (4.5 Å^3), F (7.7 Å^3), or Cl (18.8 Å^3) (see **2a**, **2c**, and **2d** as examples, Table

2). The significantly lower catalytic efficiency, yet similar turnover by *Tc*PAM of **2b** compared to those of **2a**, **2c**, and **2d** with smaller substituents suggested that the larger-size OCH_3 group through a curious pathway affected the K_M but not the turnover, like the Br group.

The catalytic efficiency (k_{cat}/K_M) of *Tc*PAM for the 4'-NO_2-substituted epoxide (**2h**) was ~2-fold higher than for the 3'-NO_2-isomer (**2g**), which parallels the difference in their turnover (k_{cat}). This regiospecificity trend was similar to that described earlier for substrates 3'-Br- (**2f**) and 4'-Br- (**2l**), where the 4'-isomer was turned over slightly faster than the 3'-isomer.

Kinetics of Isoserine Biocatalysis. To make the isoserines, the NH_2-MIO adduct needs to align the phenylpropanoid of the cinnamate epoxide for occasional amino group attack at C_β instead of at C_α (see Figure S53 of the Supporting Information for a representative AutoDock modeled conformation of **2b**). We found by LC/ESI-MS/MS analysis that *Tc*PAM converted each substituted cinnamate epoxide to an aryl*iso*serine (Figures S54–S57). Among the substituted arylisoserines, the 3'-OCH_3-phenylisoserine isomer **4b** was made most abundantly at a 37:63 ratio with its corresponding 3'-OCH_3-phenylserine **4b**, with the latter predominating (Table 2). The next most abundant arylisoserines made by *Tc*PAM were the 3'-Cl (**4e**) and 4'-CH_3 (**4i**) at ~10:90 and 40:60 ratios with their cognate arylserines **4e** and **4i**, respectively. The remaining cinnamate epoxides were converted to lesser amounts ($\leq$0.03 min^{-1}) of their isoserines (Table 2).

The sterically demanding 3'-OCH_3 substituent likely "nudged" the substrate enough to place C_β close to and in alignment with the NH_2-MIO moiety to make the 3'-OCH_3-phenylisoserine more abundantly. However, the other epoxide substrates bearing 3'-or 4'-substituents with steric volumes [NO_2 (18.2 $Å^3$), Cl (14.3 $Å^3$), CH_3 (21.3 $Å^3$) and Br (24.5 $Å^3$)] equivalent to that of OCH_3 (26.4 $Å^3$) were turned over to their isoserines less efficiently. Thus, a combination of the different steric volumes, electronics, atom geometries, and the 3' and 4'-regiochemistries of the substituents must

position the carbon skeleton of epoxides into various conformations that unpredictably promote or preclude NH_2-MIO attack at C_β. Based on the putative docked conformation of **2b** (Figure S53 of the Supporting Information), the *anti*-stereochemistry between the hydroxyl and amino groups is expected for isoserines when the epoxide is opened by S_N2 amination at C_β.

The proposed *anti*-stereoisomerism of the isoserines made enzymatically in this study is unlike the *syn*-stereochemistry of the phenylisoserine moiety found in the antineoplastic drug paclitaxel (see Scheme 1).[66] The paclitaxel pathway is presumed to proceed through a β-phenylalanyl taxane, which is hydroxylated to a penultimate phenylisoserinyl taxane intermediate,[67] but further evidence is needed to confirm this. Another report claims isolation of methyl phenylisoserinate by methanol extraction of *Taxus* plants as evidence of a putative, phenylisoserine preassembly pathway.[68] It is unclear, however, whether the phenylisoserinate ester was obtained by methanolysis of phenylisoserinyl taxanes, such as an advanced paclitaxel precursor, present in the plant. Nonetheless, if *syn*-phenylisoserine indeed occurs as a metabolite in plants, its biosynthetic pathway in *Taxus* plants remains unknown. While the *trans*-cinnamates were biocatalytically converted likely to *anti*-isoserines in this study, the results highlight cinnamate epoxides as potential naturally occurring precursors for direct amination to isoserines. We imagine that naturally occurring cinnamate, derived from phenylalanine by ammonia lyase activity in plants,[69] can be converted to cinnamate epoxide by a plant α-ketoglutarate-dependent hydroxylases. This family of nonheme Fe(II) hydroxylases convert alkenes to epoxides,[70] and specifically cinnamate to cinnamate epoxide in vitro.[71]

As noted earlier, *Tc*PAM catalyzes the isomerization of α-phenylalanine to β-phenylalanine in its natural reaction by rotating the carbon skeleton of its reaction intermediate about two bonds (see Scheme 1).[45] This rotation pathway allowed by *Tc*PAM may play a role in torqueing the ring-

opened *trans*-epoxide intermediates into a conformation needed for making *syn*-isoserine. In future studies, we look to dissect the stereoselectivity of the *Tc*PAM reaction for arylisoserine production.

CONCLUSION

The surrogate activity of *Tc*PAM catalyzed the asymmetric and regioselective transfer of an NH_2 group from a sacrificial amine group donor (2*S*)-styryl-α-alanine to racemates of cinnamate epoxide analogues in one step. *Tc*PAM made underivatized *anti*-stereoisomers of arylserines predominantly while producing significantly less of the *syn*-stereoisomer, and these observations provided valuable insights into an extended mechanism of the natural α- to β-phenylalanine isomerization reaction. The electronic effects or steric volumes of the substituents on the ring of the cinnamate epoxide substrates did not predictably change the regioselectivity of the nucleophilic attack by NH_2. Docked poses of the cinnamate epoxide racemate in *Tc*PAM suggested that the conserved Tyr80 general acid present in all other MIO enzymes[72] and proximate to the (2*R*,3*S*)-epoxide purportedly helped catalyze the more abundant (2*R*)-*anti*-arylserines. Docking analysis also identified Tyr322 as a putative general acid that likely facilitated protonation-initiated amination of the other epoxide antipode to make the lesser abundant (2*S*)-*anti*-arylserines. In addition, (2*S*)-*syn*-β-hydroxy amino acid stereoisomers are commonly found in specialized glycopeptide and depsipeptide natural products. Application of an MIO-aminomutase described here to biocatalyze enantiodivergent phenylserines with *anti*-stereoisomerism between the two chiral centers has industrial and pharmaceutical relevance, allowing the possibility to perform stereochemical structure/activity studies. For example, replacement of a naturally occurring *syn*-arylserine stereoisomer for rarer *anti*-arylserine stereoisomers in a bioactive drug candidate could increase drug bioavailability by slowing first-pass metabolism pathways or inhibiting bacterial

resistance mechanisms of bioactive compounds built on this scaffold.[73-74] Future studies will assess the stereoselectivity and stereospecificity of *Tc*PAM with enantiopure epoxide substrates for making hydroxy amino acids.

While the amino nucleophile of the loaded NH_2-MIO adduct of *Tc*PAM primarily added the NH_2 to C_α to open the epoxide substrates to their arylserines, the epoxides were also converted to their aryl*iso*serines via NH_2 attack at C_β, likely yielding the *anti*-hydroxy amino acid isomers. These biocatalyzed and underivatized bifunctional isoserines can be used as direct entry points into the synthesis of value added compounds. For example, isoserines are bioactive structural motifs of drugs such as the anticancer pharmaceutical paclitaxel and its analogues, [75-77] and a series of "KNI" HIV-1 protease inhibitors.[78] Foreseeably, the capacity of *Tc*PAM to produce isoserines from epoxides, in part, provides a starting point for us to design novel function into the enzyme.

ASSOCIATED CONTENT

Supporting Information

Spectroscopic data, materials and synthesis/characterization methods, NMR profiles, gas chromatography-mass spectrometry profiles, enzyme time-course and kinetics plots, and ligand/enzyme docking images. This material is available free of charge via the Internet at http://pubs.acs.org.

AUTHOR INFORMATION

Corresponding Author

*E-mail: walker@chemistry.msu.edu

ORCID

Kevin D. Walker: 0000-0001-5208-6692

Funding

The authors are grateful to the Michigan State University Diversity Research Network: Launch Award Program for support (GR100324-LAPKW), and to the Michigan State University AgBioResearch Grant RA078692-894.

Notes

The authors declare no competing financial interest.

ACKNOWLEDGEMENT

We thank the Michigan State University Max T. Rogers NMR Facility and the Michigan State University Research Technology Support Facility: Mass Spectrometry and Metabolomics Core for their technical assistance. We also thank Professor William Wulff for his helpful discussion on reaction mechanisms.

References:

1. Blaskovich, M. A. T., Unusual Amino Acids in Medicinal Chemistry. *J. Med. Chem.* **2016,** *59*, 10807-10836.

2. Li, R.; Wijma, H. J.; Song, L.; Cui, Y.; Otzen, M.; Tian, Y. e.; Du, J.; Li, T.; Niu, D.; Chen, Y.; Feng, J.; Han, J.; Chen, H.; Tao, Y.; Janssen, D. B.; Wu, B., Computational Redesign of Enzymes for Regio- and Enantioselective Hydroamination. *Nat. Chem. Biol.* **2018,** *14*, 664-670.

3. Wu, B.; Szymański, W.; Heberling, M. M.; Feringa, B. L.; Janssen, D. B., Aminomutases: Mechanistic Diversity, Biotechnological Applications and Future Perspectives. *Trends Biotechnol.* **2011,** *29*, 352-362.

4. Boville, C. E.; Scheele, R. A.; Koch, P.; Brinkmann-Chen, S.; Buller, A. R.; Arnold, F. H., Engineered Biosynthesis of β-Alkyl Tryptophan Analogues. *Angew. Chem. Int. Ed.* **2018,** *57*, 14764-14768.

5. Robinson, B. S.; Riccardi, K. A.; Gong, Y.-f.; Guo, Q.; Stock, D. A.; Blair, W. S.; Terry, B. J.; Deminie, C. A.; Djang, F.; Colonno, R. J.; Lin, P.-f., BMS-232632, a Highly Potent Human Immunodeficiency Virus Protease Inhibitor That Can Be Used in Combination with Other Available Antiretroviral Agents. *Antimicrob. Agents Chemother.* **2000,** *44*, 2093-2099.

6. Qian, W.-J.; Park, J.-E.; Lee, K. S.; Burke, T. R., Non-proteinogenic Amino Acids in the pThr-2 Position of a Pentamer Peptide That Confer High Binding Affinity for the Polo Box Domain (PBD) of Polo-Like Kinase 1 (Plk1). *Bioorg. Med. Chem. Lett.* **2012,** *22*, 7306-7308.

7. Zhou, H.; Xie, X.; Tang, Y., Engineering Natural Products Using Combinatorial Biosynthesis and Biocatalysis. *Curr. Opin. Biotechnol.* **2008,** *19*, 590-596.

8. Yuan, L.-F.; Li, G.-D.; Ren, X.-J.; Nian, H.; Li, X.-R.; Zhang, X.-M., Rapamycin Ameliorates Experimental Autoimmune Uveoretinitis by Inhibiting Th1/Th2/Th17 Cells and Upregulating CD4+CD25+ Foxp3 Regulatory T-Cells. *Int. J. Ophthalmol.* **2015,** *8*, 659-664.

9. Gentilucci, L.; De Marco, R.; Cerisoli, L., Chemical Modifications Designed to Improve Peptide Stability: Incorporation of Non-Natural Amino Acids, Pseudo-Peptide Bonds, and Cyclization. *Curr. Pharm. Des.* **2010,** *16*, 3185-3203.

10. Shen, Z.; Lv, C.; Zeng, S., Significance and Challenges of Stereoselectivity Assessing Methods in Drug Metabolism. *J. Pharm. Anal.* **2016,** *6*, 1-10.

11. Cao, M.; Feng, Y.; Zhang, Y.; Kang, W.; Lian, K.; Ai, L., Studies on the Metabolism and Degradation of Vancomycin in Simulated *In Vitro* and Aquatic Environment by UHPLC-Triple-TOF-MS/MS. *Sci. Rep.* **2018,** *8*, 1-13.

12. Evans, D. A.; Wood, M. R.; Trotter, B. W.; Richardson, T. I.; Barrow, J. C.; Katz, J. L., Total Syntheses of Vancomycin and Eremomycin Aglycons. *Angew. Chem. Int. Ed.* **1998,** *37*, 2700-2704.

13. Rao, A. V. R.; Gurjar, M. K.; Reddy, K. L.; Rao, A. S., Studies Directed Toward the Synthesis of Vancomycin and Related Cyclic Peptides. *Chem. Rev.* **1995,** *95*, 2135-2167.

14. Hughes, C. S.; Longo, E.; Phillips-Jones, M. K.; Hussain, R., Characterisation of the Selective Binding of Antibiotics Vancomycin and Teicoplanin by the VanS Receptor Regulating Type-A Vancomycin Resistance in the *Enterococci*. *Biochim. Biophys. Acta* **2017,** *1861*, 1951-1959.

15. Fraunfelder, F. W.; Fraunfelder, F. T., Restricting Topical Ocular Chloramphenicol Eye Drop Use in the United States. Did We Overreact? *Am. J. Ophthalmol.* **2013,** *156*, 420-422.

16. Goldstein, D. S., L-Dihydroxyphenylserine (L-DOPS): A Norepinephrine Prodrug. *Cardiovasc. Drug Rev.* **2006,** *24*, 189-203.

17. Maruyama, W.; Naoi, M.; Narabayashi, H., The Metabolism of L-DOPA and L-*threo*-3,4-Dihydroxyphenylserine and Their Effects on Monoamines in the Human Brain: Analysis of the Intraventricular Fluid from Parkinsonian Patients. *J. Neurol. Sci.* **1996,** *139*, 141-148.

18. Milanowski, D. J.; Gustafson, K. R.; Rashid, M. A.; Pannell, L. K.; McMahon, J. B.; Boyd, M. R., Gymnangiamide, a Cytotoxic Pentapeptide from the Marine Hydroid *Gymnangium regae*. *J. Org. Chem.* **2004,** *69*, 3036-3042.

19. Zhang, Y.; Farrants, H.; Li, X., Adding a Functional Handle to Nature′s Building Blocks: The Asymmetric Synthesis of β-Hydroxy-α-Amino Acids. *Chem. Asian J.* **2014,** *9*, 1752-1764.

20. Davies, S. G.; Fletcher, A. M.; Frost, A. B.; Roberts, P. M.; Thomson, J. E., Trading N and O. Part 2: Exploiting Aziridinium Intermediates for the Synthesis of β-Hydroxy-α-Amino Acids. *Tetrahedron* **2014,** *70*, 5849-5862.

21. Crich, D.; Banerjee, A., Expedient Synthesis of *syn*-β-Hydroxy-α-Amino Acid Derivatives: Phenylalanine, Tyrosine, Histidine and Tryptophan. *J. Org. Chem.* **2006,** *71*, 7106-7109.

22. Straukas, J.; Dirvianskytė, N.; Astrauskas, V.; Butkus, E., Synthesis of *N*-Arylsulfonyl DL-Phenylserine Derivatives Exhibiting Anti-Inflammatory Activity in Experimental Studies. *Farmaco* **2002,** *57*, 803-808.

23. Zhang, Y.; Xu, C.; Lam, H. Y.; Lee, C. L.; Li, X., Protein Chemical Synthesis by Serine and Threonine Ligation. *Proc. Natl. Acad. Sci. U.S.A.* **2013,** *110*, 6657-6662.

24. Leblond, B.; Beausoleil, E.; Taverne, T.; Donello, J. E. Heterocyclyl-3-Hydroxy-2-Amino-Propionic Acid Amides and Related Compounds Having Analgesic and/or Immunostimulant Activity. WO 2006/081273A1, 2006.

25. Donello, J. E.; Schweighoffer, F. J.; Leblond, B. Methods for Treating Chronic Pain Using 3-Aryl-3-Hydroxy-2-Amino-Propionic Acid Amides, 3-Heteroaryl-3-Hydroxy-2-Amino-Propionic Acid Amides and Related Compounds. WO 2008/011478, 2008.

26. Ambrus, G. F.; Kurjan, K. C.; Zanon, J.; Libralon, G.; Faveri, C. D. (−)-(2*R*,3*S*)-2-Amino-3-Hydroxy-3-Pyridin-4-yl-1-Pyrrolidin-1-yl-Propan-1-one (L)-(+) Tartrate Salt, Its Method of Production and Use. WO 2015/023816A1, 2015.

27. Schmidt, M. A.; Reiff, E. A.; Qian, X.; Hang, C.; Truc, V. C.; Natalie, K. J.; Wang, C.; Albrecht, J.; Lee, A. G.; Lo, E. T.; Guo, Z.; Goswami, A.; Goldberg, S.; Pesti, J.; Rossano, L. T., Development of a Two-Step, Enantioselective Synthesis of an Amino Alcohol Drug Candidate. *Org. Process Res. Dev.* **2015,** *19*, 1317-1322.

28. Fan, S.; Liu, S.; Zhang, H.; Liu, Y.; Yang, Y.; Jin, L., Biocatalytic Synthesis of Enantiopure β-Methoxy-β-arylalanine Derivatives. *Eur. J. Org. Chem.* **2014,** *2014*, 5591-5597.

29. Duckers, N.; Baer, K.; Simon, S.; Groger, H.; Hummel, W., Threonine Aldolases-Screening, Properties and Applications in the Synthesis of Non-Proteinogenic β-Hydroxy-α-Amino Acids. *Appl. Microbiol. Biotechnol.* **2010,** *88*, 409-424.

30. Hernandez-Juan, F. A.; Richardson, R. D.; Dixon, D. J., A Stereoselective Oxy-Michael Route to Protected β-Aryl-β-Hydroxy-α-Amino Acids. *Synlett* **2006,** *2006*, 2673-2675.

31. Guanti, G.; Banfi, L.; Narisano, E., Enantiospecific and Diastereoselective Synthesis of Anti α-Hydrazino- And α-Amino-β-Hydroxyacids through "Electrophilic Amination" of β-Hydroxyesters. *Tetrahedron* **1988,** *44*, 5553-5562.

32. Li, G.; Chang, H.-T.; Sharpless, K. B., Catalytic Asymmetric Aminohydroxylation (AA) of Olefins. *Angew. Chem. Int. Ed.* **1996,** *35*, 451-454.

33. Schollkopf, U., Asymmetric Syntheses of Amino Acids via Metalated Bis-Lactim Ethers of 2,5-Diketopiperazines. *Pure Appl. Chem.* **1983,** *55*, 1799-1806.

34. Challener, C. A., Going Green with Biocatalysis. *Pharm. Technol.* **2016,** *40*, 24-25.

35. Challener, C. A., Synthetic Biology: The Next Frontier in Chiral Chemistry for API Synthesis. *Pharm. Technol.* **2014,** *38*, 36-40.

36. Williams, G.; Hall, M., Eds. *Modern Biocatalysis: Advances Towards Synthetic Biological Systems*. The Royal Society of Chemistry: London, United Kingdom, 2018.

37. Zawodny, W.; Marshall, J. R.; Finnigan, J. D.; Turner, N. J.; Clayden, J.; Montgomery, S. L., Chemoenzymatic Synthesis of Substituted Azepanes by Sequential Biocatalytic Reduction and Organolithium-Mediated Rearrangement. *J. Am. Chem. Soc.* **2018,** *140*, 17872-17877.

38. Wen, W.; Chen, L.; Luo, M.-J.; Zhang, Y.; Chen, Y.-C.; Ouyang, Q.; Guo, Q.-X., Chiral Aldehyde Catalysis for the Catalytic Asymmetric Activation of Glycine Esters. *J. Am. Chem. Soc.* **2018,** *140*, 9774-9780.

39. The Cahn-Ingold-Prelog (CIP) (*R*,*S*) convention is use here instead of the older D/L conventions to assign the absolute configuration at the α-carbon of the β-hydroxy α-amino acids. CIP rules are used also to describe the product selectivity of a TA based on the stereochemistry of the α-carbon. The *syn*/*anti* are used instead of *threo*/*erythro*-diastereomeric descriptors, respectively, to designate the relative stereochemistry at the α- and β-carbons in the zigzag configuration.

40. Baer, K.; Duckers, N.; Rosenbaum, T.; Leggewie, C.; Simon, S.; Krausser, M.; Osswald, S.; Hummel, W.; Groger, H., A Study towards Efficient L-Threonine Aldolase-Catalyzed Enantio-

and Diastereoselective Aldol Reactions of Glycine with Substituted Benzaldehydes: Biocatalyst Production and Process Development. *Tetrahedron: Asymmetry* **2011,** *22*, 925-928.

41. Liu, J. Q.; Odani, M.; Yasuoka, T.; Dairi, T.; Itoh, N.; Kataoka, M.; Shimizu, S.; Yamada, H., Gene Cloning and Overproduction of Low-Specificity D-Threonine Aldolase from *Alcaligenes xylosoxidans* and Its Application for Production of a Key Intermediate for Parkinsonism Drug. *Appl. Microbiol. Biotechnol.* **2000,** *54*, 44-51.

42. Walker, K. D.; Klettke, K.; Akiyama, T.; Croteau, R., Cloning, Heterologous Expression, and Characterization of a Phenylalanine Aminomutase Involved in Taxol Biosynthesis. *J. Biol. Chem.* **2004,** *279*, 53947-53954.

43. Steele, C. L.; Chen, Y.; Dougherty, B. A.; Li, W.; Hofstead, S.; Lam, K. S.; Xing, Z.; Chiang, S. J., Purification, Cloning, and Functional Expression of Phenylalanine Aminomutase: The First Committed Step in Taxol Side-Chain Biosynthesis. *Arch. Biochem. Biophys.* **2005,** *438*, 1-10.

44. Verkuijl, B. J. V.; Szymanski, W.; Wu, B.; Minnaard, A. J.; Janssen, D. B.; de Vries, J. G.; Feringa, B. L., Enantiomerically Pure β-Phenylalanine Analogues from α/β-Phenylalanine Mixtures in a Single Reactive Extraction Step. *Chem. Commun.* **2010,** *46*, 901-903.

45. Feng, L.; Wanninayake, U.; Strom, S.; Geiger, J.; Walker, K. D., Mechanistic, Mutational, and Structural Evaluation of a *Taxus* Phenylalanine Aminomutase. *Biochemistry* **2011,** *50*, 2919-2930.

46. Montavon, T. J.; Christianson, C. V.; Festin, G. M.; Shen, B.; Bruner, S. D., Design and Characterization of Mechanism-Based Inhibitors for the Tyrosine Aminomutase *Sg*TAM. *Bioorg. Med. Chem. Lett.* **2008,** *18*, 3099-3102.

47. Strom, S.; Wanninayake, U.; Ratnayake, N. D.; Walker, K. D.; Geiger, J. H., Insights into the Mechanistic Pathway of the *Pantoea agglomerans* Phenylalanine Aminomutase. *Angew. Chem. Int. Ed.* **2012,** *51*, 2898-2902.

48. Wanninayake, U.; Walker, K. D., Assessing the Deamination Rate of a Covalent Aminomutase Adduct by Burst Phase Analysis. *Biochemistry* **2012,** *51*, 5226-5228.

49. Wanninayake, U.; Deporre, Y.; Ondari, M.; Walker, K. D., (*S*)-Styryl-α-Alanine Used to Probe the Intermolecular Mechanism of an Intramolecular MIO-Aminomutase. *Biochemistry* **2011,** *50*, 10082-10090.

50. Corey, P. F.; Ward, F. E., Buffered Potassium Peroxymonosulfate-Acetone Epoxidation of α,β-Unsaturated Acids. *J. Org. Chem.* **1986,** *51*, 1925-1926.

51. Smolarsky, M.; Koshland, D. E., Inactivation of the Opiate Receptor in Bovine Caudate Nucleus by Azide Enkephalin Analogs. *J. Biol. Chem.* **1980,** *255*, 7244-7249.

52. Wu, B.; Szymański, W.; Wybenga, G. G.; Heberling, M. M.; Bartsch, S.; de Wildeman, S.; Poelarends, G. J.; Feringa, B. L.; Dijkstra, B. W.; Janssen, D. B., Mechanism-Inspired Engineering of Phenylalanine Aminomutase for Enhanced β-Regioselective Asymmetric Amination of Cinnamates. *Angew. Chem. Int. Ed.* **2012,** *51*, 482-486.

53. Szymanski, W.; Wu, B.; Weiner, B.; de Wildeman, S.; Feringa, B. L.; Janssen, D. B., Phenylalanine Aminomutase-Catalyzed Addition of Ammonia to Substituted Cinnamic Acids: A Route to Enantiopure α- and β-Amino Acids. *J. Org. Chem.* **2009,** *74*, 9152-9157.

54. Srivastava, R. P.; McChesney, J. D., A Practical and Inexpensive Synthesis of the Taxol C-13 Side Chain; *N*-Benzoyl-(2*R*,3*S*)-3-Phenylisoserine. *Nat. Prod. Lett.* **1995,** *6*, 147-152.

55. Hammett, L. P., The Effect of Structure upon the Reactions of Organic Compounds. Benzene Derivatives. *J. Am. Chem. Soc.* **1937,** *59*, 96-103.

56. Feske, B. D.; Kaluzna, I. A.; Stewart, J. D., Enantiodivergent, Biocatalytic Routes to Both Taxol Side Chain Antipodes. *J. Org. Chem.* **2005,** *70*, 9654-9657.

57. Futagawa, S.; Inui, T.; Shiba, T., Nuclear Magnetic Resonance Study of the Stereoisomeric 2-Oxazolidone and 2-Phenyl-2-Oxazoline Derivatives of α-Amino-β-Hydroxy Acids. *Bull. Chem. Soc. Jpn.* **1973,** *46*, 3308-3310.

58. Liu, J.-Q.; Dairi, T.; Itoh, N.; Kataoka, M.; Shimizu, S.; Yamada, H., Gene Cloning, Biochemical Characterization and Physiological Role of a Thermostable Low-Specificity L-Threonine Aldolase from *Escherichia coli*. *Eur. J. Biochem.* **1998,** *255*, 220-226.

59. Pettersen, E. F.; Goddard, T. D.; Huang, C. C.; Couch, G. S.; Greenblatt, D. M.; Meng, E. C.; Ferrin, T. E., UCSF Chimera - A Visualization System for Exploratory Research and Analysis. *J. Comput. Chem.* **2004,** *25*, 1605-1612.

60. Trott, O.; Olson, A. J., AutoDock Vina: Improving the Speed and Accuracy of Docking with a New Scoring Function, Efficient Optimization, and Multithreading. *J. Comput. Chem.* **2010,** *31*, 455-461.

61. Wybenga, G. G.; Szymanski, W.; Wu, B.; Feringa, B. L.; Janssen, D. B.; Dijkstra, B. W., Structural Investigations into the Stereochemistry and Activity of a Phenylalanine-2,3-Aminomutase from *Taxus chinensis*. *Biochemistry* **2014,** *53*, 3187-3198.

62. Hariharan, V. A.; Denton, T. T.; Paraszcszak, S.; McEvoy, K.; Jeitner, T. M.; Krasnikov, B. F.; Cooper, A. J. L., The Enzymology of 2-Hydroxyglutarate, 2-Hydroxyglutaramate and 2-Hydroxysuccinamate and Their Relationship to Oncometabolites. *Biology* **2017,** *6*, 24.

63. Lohman, J. R.; Shen, B. 4-Methylideneimidazole-5-One-Containing Aminomutases in Enediyne Biosynthesis. In *Methods Enzymol.*, Hopwood, D. A., Ed. Academic Press: 2012; Vol. 516, pp 299-319.

64. Connolly, M. L., The Molecular Surface Package. *J. Mol. Graphics* **1993,** *11*, 139-141.

65. Thornburg, C. K.; Wortas-Strom, S.; Nosrati, M.; Geiger, J. H.; Walker, K. D., Kinetically and Crystallographically Guided Mutations of a Benzoate CoA Ligase (BadA) Elucidate Mechanism and Expand Substrate Permissivity. *Biochemistry* **2015,** *54*, 6230-6242.

66. Galla, Z.; Beke, F.; Forró, E.; Fülöp, F., Enantioselective Hydrolysis of 3,4-Disubstituted β-Lactams. An Efficient Enzymatic Method for the Preparation of a Key Taxol Side-Chain Intermediate. *J. Mol. Catal. B: Enzym.* **2016,** *123*, 107-112.

67. Long, R. M.; Croteau, R., Preliminary Assessment of the C13-Side Chain 2'-Hydroxylase Involved in Taxol Biosynthesis. *Biochem. Biophys. Res. Commun.* **2005,** *338*, 410-417.

68. Tachibana, S.; Watanabe, E.; Ueno, J.; Tokubuchi, K.; Itoh, K., Isolation of Phenylisoserine Methyl Ester from the Leaves of *Taxus cuspidata* var. *nana*. *J. Wood Sci.* **2005,** *51*, 176-180.

69. Camm, E. L.; Towers, G. H. N., Phenylalanine Ammonia Lyase. *Phytochemistry* **1973,** *12*, 961-973.

70. Farrow, S. C.; Facchini, P. J., Functional Diversity of 2-Oxoglutarate/Fe(II)-Dependent Dioxygenases in Plant Metabolism. *Front. Plant Sci.* **2014,** *5*, 1-15.

71. Griffin, S. L.; Godbey, J. A.; Oman, T. J.; Embrey, S. K.; Karnoup, A.; Kuppannan, K.; Barnett, B. W.; Lin, G.; Harpham, N. V. J.; Juba, A. N.; Schafer, B. W.; Cicchillo, R. M., Characterization of Aryloxyalkanoate Dioxygenase-12, a Nonheme Fe(II)/α-Ketoglutarate-Dependent Dioxygenase, Expressed in Transgenic Soybean and *Pseudomonas fluorescens*. *J. Agric. Food. Chem.* **2013,** *61*, 6589-6596.

72. Attanayake, G.; Walter, T.; Walker, K. D., Understanding Which Residues of the Active Site and Loop Structure of a Tyrosine Aminomutase Define Its Mutase and Lyase Activities. *Biochemistry* **2018,** *57*, 3503-3514.

73. Wang, X.; Zheng, M.; Liu, J.; Huang, Z.; Bai, Y.; Ren, Z.; Wang, Z.; Tian, Y.; Qiao, Z.; Liu, W.; Feng, F., Differences of First-Pass Effect in the Liver and Intestine Contribute to the Stereoselective Pharmacokinetics of Rhynchophylline and Isorhynchophylline Epimers in Rats. *J. Ethnopharmacol.* **2017,** *209*, 175-183.

74. Bhateria, M.; Rachumallu, R.; Yerrabelli, S.; Saxena, A. K.; Bhatta, R. S., Insight into Stereoselective Disposition of Enantiomers of a Potent Antithrombotic Agent, S002-333 Following Administration of the Racemic Compound to Mice. *Eur. J. Pharm. Sci.* **2017,** *101*, 107-114.

75. Yang, C. H.; Wang, C.; Ojima, I.; Horwitz, S. B., Taxol Analogues Exhibit Differential Effects on Photoaffinity Labeling of β-Tubulin and the Multidrug Resistance Associated P-Glycoprotein. *J. Nat. Prod.* **2018,** *81*, 600-606.

76. Baloglu, E.; Hoch, J. M.; Chatterjee, S. K.; Ravindra, R.; Bane, S.; Kingston, D. G., Synthesis and Biological Evaluation of C-3'NH/C-10 and C-2/C-10 Modified Paclitaxel Analogues. *Biorg. Med. Chem.* **2003,** *11*, 1557-1568.

77. Baloglu, E.; Kingston, D. G., The Taxane Diterpenoids. *J. Nat. Prod.* **1999,** *62*, 1448-1472.

78. Hamada, Y.; Kiso, Y., New Directions for Protease Inhibitors Directed Drug Discovery. *Pept. Sci.* **2016,** *106*, 563-579.

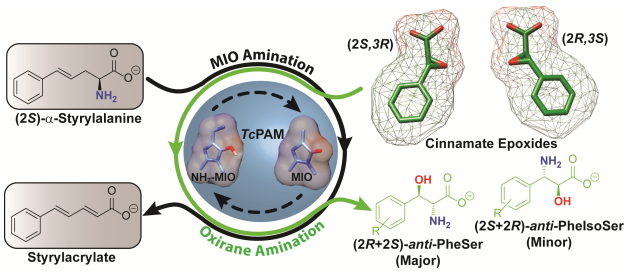
(2S)-α-Styrylalanine
MIO Amination
(2S,3R)
(2R,3S)
Cinnamate Epoxides
TcPAM
NH2-MIO
MIO
Styrylacrylate
Oxirane Amination
(2R+2S)-anti-PheSer
(Major)
(2S+2R)-anti-PheIsoSer
(Minor)